Article

Dual-target CAR-Ts with on- and off-tumour activity may override immune suppression in solid cancers: A mathematical proof of concept

Odelaisy León-Triana [1], Antonio Pérez-Martínez[2], Manuel Ramírez-Orellana[3], Víctor M. Pérez-García [4]

[1] Mathematical Oncology Laboratory (MOLAB), Department of Mathematics and Instituto de Matemática Aplicada a la Ciencia y la Ingeniería, Universidad de Castilla-La Mancha. Avda. Camilo José Cela, 3, 13071 Ciudad Real; odelaisy.leon@uclm.es

[2] Paediatric Haemato-Oncology Department, Hospital Universitario La Paz, Madrid, Spain.

[3] Translational Research Unit in Paediatric Haemato-Oncology, Haematopoietic Stem Cell Transplantation and Cell Therapy, Hospital Universitario La Paz, Madrid, Spain.

[4] Mathematical Oncology Laboratory (MOLAB), Department of Mathematics and Instituto de Matemática Aplicada a la Ciencia y la Ingeniería, Universidad de Castilla-La Mancha. Avda. Camilo José Cela, 3, 13071 Ciudad Real; victor.perezgarcia@uclm.es

* Correspondence: victor.perezgarcia@uclm.es

Abstract: Chimeric antigen receptor (CAR)-T cell-based therapies have achieved substantial successes against B-cell malignancies, what has led to a growing scientific and clinical interest on extending their use to solid cancers. However, results for solid tumours have been limited up to now, in part due to the immuno-suppressive tumour microenvironment, that is able to inactivate CAR-T cell clones. In this paper we put forward a mathematical model describing the competition of CAR-T and tumour cells, accounting for their immunosuppressive capabilities. Using the mathematical model, we show that the use of large numbers of CAR-T cells targeting the solid tumour antigens could overcome the cancer immunosuppressive potential. To achieve such high levels of CAR-T cells we propose and study computationaly, the manufacture and injection of CAR-T cells targeting two antigens: CD19 and a tumour-associated antigen. We study in-silico the resulting dynamics of the disease after the injection of this product and find that the expansion of the CAR-T cell population in the blood and lymphopoietic organs could lead to the massive generation of an army of CAR-T cells targetting the solid tumour, and potentially overcoming its inmune suppression capabilities. That strategy could benefit from the combination with PD-1 inhibitors and of low tumour loads. Our computational results provide a theoretical support for the treatment of different types of solid tumours using T-cells engineered with combination treatments of dual CARs with on- and off-tumour activity and anti-PD1 drugs after completion of classical cytoreductive treatments.

Keywords: Mathematical oncology; CAR-T cells; mathematical immunology; mathematical modelling; immunotherapy of solid tumours; glioblastoma

PACS: 05.45.-a; 87.17.Aa; 87.17.Ee; 87.18.-h; 87.18.Nq; 87.19.xj

MSC: 92-10; 92C32; 92C45; 34C60

1. Introduction

Chimeric antigen receptor (CAR) T-cells are modified autologous or allogeneic T cells. Their extracellular domain is engineered to recognize a tumour associated antigen and the intracellular domain contains a T cell activation signal. Upon CAR engagement of the associated antigen, primary T-cell activation occurs and leads to cytokine release, cytolytic degranulation, resulting in the target cell death, and T-cell proliferation [1].

Preprints (www.preprints.org) | NOT PEER-REVIEWED | Posted: 7 December 2020 doi:10.20944/preprints202012.0166.v1

CAR-T cells engineered to recognize $CD19^+$ cells have been successfully to treat B-cell malignancies. Remarkable sucesses have been achieved in Acute Lymphoblastic Leukaemia patients [1–4]. Furthermore, good results have also been reported for multiple myelomas [5] and diffuse large B-cell lymphoma [6], and also in refractory acute myeloid leukaemia using CD33- specific CART cells [7]. These successes have motivated the study of the applicability of CAR-T cell therapies against solid tumours [8], and led to ongoing clinical trials for a variety of cancers including glioblastomas, gastrointestinal cancers, genitourinary cancers, breast cancers, lung cancers, and others [9]. However, CAR-T cell treatments of solid tumours face significant challenges. The first one is the identification of suitable tumour antigens expressed only on cancerous but not on healthy cells, i.e. limiting the on-target off-tumour activity of the product [10]. It is also necessary that the antigens selected for the therapy be humanized, to avoid the generation of antibodies that block the CAR-T [11]. Other major issues include T-cell persistence and expansion, T-cell trafficking into tumours, and immune resistance mechanisms that may define the ultimate fate of CAR-T cells [12].

Due to the above mentioned reasons, it is essential to develop strategies improving the effectiveness of therapy [13]. Combined CAR targeting has been explored as a way to improve antigen recognition and limit the possibility of tumour escape [14,15]. Several pre-clinical studies have evaluated the simultaneous targeting of two tumour-restricted antigens [16,17] and sequential treatments as CAR-T cocktails [18]. One of the main multi-antigen-targeted CAR-T cell therapies under study is dual CAR-T cells, where individual T cells are engineered to co-express two separate CARs specific for cognate antigens.

Mathematical modelling has the potential to help in finding optimal administration protocols, provide a deeper understanding of the dynamics, help in the design of clinical trials and more [19,20]. Some recent mathematical modelling studies have been performed studying different aspects of CAR-T cell therapies [21–28]. In this paper we study in-silico, using a mathematical model, the response of a solid tumour to a dual CAR-T product targeting both CD19 and a tumour-associated antigen. Our idea, to be explored computationally, is using B-cells expressing the CD19 antigen to amplify the CAR-T population in-patient what may allow for substantially higher levels of CAR-T cells attacking on the tumour, thus helping to overcome the tumour immunosuppressive capabilities.

In this paper we will take glioblastoma (GBM) as specific example, but the concept explored here could be applied to different cancer types without substantial modifications. Different tumour antigens that have been targeted in CAR-T clinical trials in GBM include IL-13Ra2, EGFRvIII, and Her2 [29]. The main obstacles for CAR-T therapies in GBM are antigen escape due to tumour immunosuppression, heterogeneous expression of identified tumour antigens and toxicity problems [25,30].

The results of trial studies with IL13Rα2 on GBM are encouraging regarding safety and penetrance of CAR-T cells [31,32]. Persistence of CAR-T cells was evidenced in that study, as it was the fast increase in endogenous immune cells and inflammatory cytokines after each infusion. Also, a study with CAR-T cells targeting EGFRvIII demonstrated transient expansion of CAR-T cells and traffic to the brain and regions of active GBM [33].

Our plan in this paper is as follows. First, in Sec. 2 we present the mathematical models to be used through the paper and discuss how to parametrize them. Next, in Sec. 3 we present the results of our computer simulations of the situation where CAR-T cells are injected bearing a single CAR group targetting a immunosuppressive tumour. Simulations of the outcome of the therapy with CAR-T cells with dual CAR groups, targeting the tumour antigen and an off-tumour antigen (CD19) are presented in Sec. 4. Finally, in Sec. 5 we discuss the implications of the results and Sec. 6 summarizes our conclusions. Some theoretical results on the model equations properties are presented in Appendixes A and B.

Preprints (www.preprints.org) | NOT PEER-REVIEWED | Posted: 7 December 2020 doi:10.20944/preprints202012.0166.v1

2. Mathematical models

2.1. Model of solid tumour response to a CAR-T cell treatment in the presence of immune suppression

A first mathematical model to be used in this paper describes the competition between a tumour population $T(t)$ and CAR-T cells $C(t)$ neglecting spatial aspects and other componetns of the immune system. The equations of our model read

$$\frac{dC}{dt} = \frac{\rho_C CT}{g_T + T} - \frac{\alpha_1 CT}{g_C + C} - \frac{1}{\tau_C} C, \tag{1a}$$

$$\frac{dT}{dt} = \rho_T T - \alpha_2 CT. \tag{1b}$$

The first term in Eq. (1a) accounts for the stimulation of CAR-T cell proliferation after encounters with tumour cells with a rate constant ρ_C and a typical saturation population of the order of g_T [34]. The second term describes the inactivation of CAR-T cells by tumour cells with a maximal inactivation rate α_1 per tumour cell, and a typical cellular saturation level around g_C CAR-T cells. The last term in Eq. (1a) describes the natural death (or inactivation) of activated CAR-T cells. Eq. (1b) describes the dynamics of tumour cells, with the first term accounting for proliferation (with rate ρ_T) and the second one accounting for tumour cell killing by the CAR-T cells with a rate α_2.

Appendix A contains some mathematical results on the existence, uniqueness, positiveness of solutions of Eqs. (1) as well as on the stability of its critical points.

2.2. Modelling CAR-T cells targetting on-tumour and off-tumour antigens

A second model to be used in this paper accounts for CAR-T cells with dual CAR groups targeting two different antigens. As an example, for the case of GBM the tumour-associated antigen could be IL-13Rα2, which is associated with a bad prognosis and over-expressed in $> 60\%$ of those tumours but not on normal brain tissue [35]. This antigen will be assumed to be present homogeneously in the population of tumour cells. The second antigen will be expressed by a normal tissue, whose elimination would be assumed to be compatible with life. In this paper we will think of this second antigen as being CD19, expressed by B cells. However, the same ideas should be applicable to other antigens owned by a normal cell population whose eradication does not compromise patient survival.

When the therapy is delivered intravenously, CAR-T cells will be initially amplified upon their encounters with $CD19^+$ cells in peripheral blood and in the bone marrow and will also traffic to the tumour sites.

Let $C(t)$, $\bar{C}(t)$, $B(t)$ and $T(t)$ be nonnegative time-varying functions accounting for the number of CAR-T cells out of the tumour site, CAR-T cells on the tumour site, normal cells expressing the second antigen (in our case, B cells) and tumour cells, respectively. A simplified set of equations describing the dynamics of these populations is

$$\frac{d\bar{C}}{dt} = \frac{\rho_{\bar{C}} \bar{C} B}{g_B + B} - \frac{1}{\tau_C} \bar{C} - k\bar{C}, \tag{2a}$$

$$\frac{dB}{dt} = -\alpha_B B\bar{C} - \frac{1}{\tau_B} B, \tag{2b}$$

$$\frac{dC}{dt} = k\bar{C} + \frac{\rho_C CT}{g_T + T} - \frac{\alpha_1 CT}{g_C + C} - \frac{1}{\tau_C} C, \tag{2c}$$

$$\frac{dT}{dt} = \rho_T T - \alpha_2 CT. \tag{2d}$$

Eqs. (2a-2b) describe the off-tumour interaction between CAR-T and B cells as in previous works [26]. The first term in Eq. (2a), represents B cell-induced CAR-T proliferation. The second

 doi:10.20944/preprints202012.0166.v1

term represents natural cell death, where τ_C is the activated CAR-T lifespan. Finally, the term $-k\bar{C}$ represents the traffic of CAR-T cells to brain areas having active GBM cells, where $0 < k < 1$ is the average fraction of CAR-T cells crossing the blood-brain barrier (BBB) and infiltrating the tumour site.

The CAR-T effect on B cell growth is included in this model through the term $-\alpha_B B\bar{C}$ in Eq. (2b), which represents the rate of CAR-T cell induced B cell death. The mean lifetime of B cells is described by τ_B in the last term of Eq. (2b). Since we deal mostly with the short term dynamics after the injection of the CAR-T cells, we will not include the production of B cells in the bone and its potential contribution of the hematopoietic compartments to the continuous activation of the CAR-T population.

Eqs (2c-2d) are inspired in the Kuznetsov model [36] and describe the response of effector cells to the growth of tumour cells. The CAR-T cells that get to the tumour region, described by Eq. (2c), are stimulated by target cells $T(t)$. The stimulation rate $\rho_C CT/(g_T + T)$ accounts for the increase in CAR-T proliferation due to the encounters with tumour cells and has a maximum value of ρ_C as T gets large. CAR-T cells are killed or inactivated by tumour cells $T(t)$ with a rate α_1 and are assumed to have a finite lifespan τ_C. Tumour cells [Eq. (2d)] proliferate with a rate ρ_T and die due to the encounters with the CAR-T cells with a rate α_2.

Thus, the biological effects ruling the dynamics of CAR-T cells in this mathematical model are: migration to the tumour site, stimulation by the antigens, natural cell death, and inactivation by the tumour cells. The sum of $\bar{C}(t)$ and $C(t)$ represents the total number of CAR-T cells at time t.

The theoretical study of existence and uniqueness of solutions of Eqs. (2), together with some results on the stability of the critical points, are presented in Appendix B.

2.3. Parameter estimation

The proposed models have several parameters to estimate. The maximum mitotic rate ρ_C and $\rho_{\bar{C}}$, related to the stimulation effect of the T cells by the interaction with the targets (CD 19^+ or tumour antigen), will depend on the properties of the CAR-T product. These parameters will be taken in the range 0.2-0.9 day^{-1} according to the values reported in other models [26,37] and in agreement with the fact that stimulated CAR-T cells can perform a few mitotic divisions per day. For current CAR-T products the mean lifetime τ_C of activated CAR T cells is in the range of 1-4 weeks [38]. To estimate the tumour inactivation rate, we relied on the inhibitory role of PD-1 in immune responses [39]. A biologically broad range of values has been explored for the maximum tumour inactivation rate α_1 in the range 0.01 to 0.99 day^{-1}. This number has been estimated from tumour growth data in previous works. For instance the c parameter in Ref. [40] satisfies roughly $c = 10^{-11}$ day^{-}1 cell$^{-1} \sim \alpha_1/g_C$ what leads to a maximum value of $\alpha_1 \sim 0.05$, taking for g_C the typical levels of T cells in blood. The value of α_1 would be substantially smaller by a factor between 10 and 10^3 under the action of anti PD-1 treatments [41,42]. The biochemical process of T-cell inactivation by tumour cells could be much faster. Larger values could also be possible biologically, however we will assume that for tumours with very high immunosuppressive capabilities PD-1 inhibitors could be used as adjuvant treatment to take α_1 into the range of values studied [43].

Glioblastomas are fast-growing malignant primary brain tumours with proliferation rate ρ_T on the order of several weeks, but have considerable variation in growth rates between individual patients [44]. Thus we will take ρ_T to be in the range 0.001-0.2 day^{-1}.

We assume that CAR-T cells have similar killing efficiency against both the tumour (α_2) and CD19$^+$ cells (α_B), with values around 10^{-11} day^{-1} [45]. B-cell lymphocyte lifetime τ_B is known to be about 5-6 weeks [46]. We will assume that in dual therapy, CAR-T cells are injected after lymphoid depletion treatment to promote expansion of CAR-T by stimulation with B cells as usual. We set the initial number of B lymphocytes to be 2.5 $\times 10^{10}$ to account for the effect of this treatment [26].

Finally, the values of g_T and g_B indicate the inflection points from which the rate of stimulation of CAR-T cells increases and are related to the antigen levels. These constants have been estimated in previous works by adjusting the data in experiments with mice [36]. In our case, because of the lack of experimental results on the dual CAR-Ts proposed here we estimated them using the model (1) and

Preprints (www.preprints.org) | NOT PEER-REVIEWED | Posted: 7 December 2020 doi:10.20944/preprints202012.0166.v1

Parameter	Description	Value	Units	Source
ρ_C	Mitotic stimulation of CAR-T cells by tumour cells	$0.2 - 0.9$	day^{-1}	[26,37]
g_T	T cells concentration for half-maximal CAR-T cell proliferation	10^{10}	cell	Estimated from [37]
α_1	Tumour inactivation rate	$0.01 - 0.99$	day^{-1}	[40]
g_C	CAR-T concentration for half-maximal tumour inactivation	$5 \times 10^8 - 5 \times 10^9$	cell	Estimated from [40]
τ_C	Activated CAR-T cell lifetime	$7 - 30$	day	[38]
ρ_T	Tumour growth rate	$(0.001 - 0.2)$	day^{-1}	[44]
α_2	Killing efficiency of CAR-T cells against tumour	$\sim 10^{-11}$	day^{-1} $\times$ cell^{-1}	[26]
$\rho_{\bar{C}}$	Mitotic stimulation of CAR-T cells by CD19$^+$	$(0.2 - 0.9)$	day^{-1}	[26,37]
g_B	B cells concentration for half-maximal CAR-T cell proliferation	10^{10}	cell	Estimated from [37]
τ_B	B-lymphocyte lifetime	$30 - 60$	day	[46]
α_B	Killing efficiency of CAR-T cells against CD19$^+$ cells	$\sim 10^{-11}$	day^{-1} $\times$ cell^{-1}	Estimated from [45]

Table 1. Parameter values for model Eqs. (1) and (2).

the results obtained in Ref. [37] (stimulation rate, the maximum of transgenic copies of tisagenlecleucel, and the time of peak expansion of CAR-T cells). To do so, we neglected the immune suppression term, that is not present in leukaemias and the parameters related to the type of cancer were chosen as in Ref. [26]. We obtained values of g_T and g_B around 1-2 $\times 10^{10}$ cell.

A summary of the model parameters and their numerical values is given in Table 1.

Preprints (www.preprints.org) | NOT PEER-REVIEWED | Posted: 7 December 2020 doi:10.20944/preprints202012.0166.v1

3. Results (I): Therapy outcomes under immune suppression using CAR-T cells with a single CAR group targetting a tumour antigen.

3.1. A high level of immune suppression prevents in-patient expansion of CAR-T cells

Firstly, we studied the effect of the inmunosuppressive strength of tumour cells as measured by α_1, on the dynamics of model Eq. (1). Let us note that in Eq. (1a), the term proportional to α_1 plays the role of a CAR-T cell growth inhibition. When immunosuppression is neglected, i.e. $\alpha_1 = 0$, an initial condition C_0 can always be found such that the treatment induces an initial reduction of the total number of tumour cells, i.e., $T(t)$ would initially decrease, allowing for tumour control for long times. Using Eq. (1b) and the condition $dT/dt < 0$ it is easy to obtain that the condition for the therapy to be initially effective is $C(t) > \rho_T/\alpha_2$.

Figure 1(a,c) provides an example of an effective therapy in the absence of tumour-mediated immunosuppression. An initial dose of $C_0 = 8 \times 10^7$ CAR-T cells, sufficed to reduce the tumour burden below observable limits in a few weeks.

Next, we studied the tumour response to CAR-T cell infusion in the presence of tumour immune suppression, i.e. for values of $\alpha_1 > 0$. Tumour control was also obtained for small α_1 values (see Figure 1(a,c)), where the CAR-T population overcame the immune suppression and grew, promoting the death of a large number of tumour cells. The expansion of the CAR-T cell population was slower than in the case $\alpha_1 = 0$ and the reduction of the tumour load also occurred on longer time scale, but tumour control was also achieved in this situation of low α_1 values corresponding to tumours with low immunosuppressive strength.

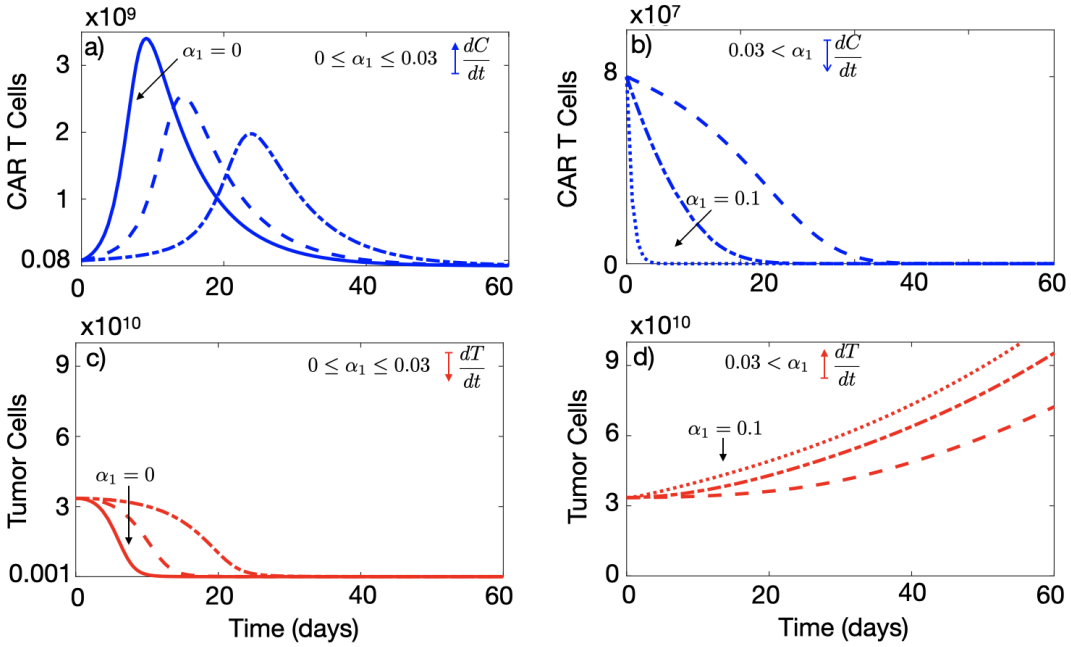

Figure 1. Tumour immune suppression rules the expansion of the CAR-T cells *in-silico*. Dynamics of the number of CAR-T (blue curves) and tumour cells (red curves) ruled by Eq. (1) in different immunosuppression scenarios. Subplots (a, c) show the results for $\alpha_1 = 0$ (solid lines), $\alpha_1 = 0.02$ day^{-1} (dashed lines) and $\alpha_1 = 0.03$ day^{-1}(dash-dotted lines) and subplots (b,d) for $\alpha_1 = 0.035$ day^{-1}(dashed lines), $\alpha_1 = 0.04$ day^{-1}(dash-dotted lines) and $\alpha_1 = 0.1$ day^{-1}(dotted lines). Initial data used in the simulations $C_0 = 8 \times 10^7$ cells, $T_0 = 3.35 \times 10^{10}$ cells and parameter values $\tau_C = 7$ days, $\rho_C = 0.9$ day^{-1}, $\rho_T = 1/50$ day^{-1}, $\alpha_2 = 2.5 \times 10^{-10}$ day^{-1} cell^{-1}, $g_T = 10^{10}$ and $g_C = 2 \times 10^9$.

We can also see in Figure 1(b,d) that when the value of the immunosuppression parameter was increased beyond the threshold $\alpha_1 > 0.03$, the tumour and CAR-T cell dynamics changed substantially.

Preprints (www.preprints.org) | NOT PEER-REVIEWED | Posted: 7 December 2020 doi:10.20944/preprints202012.0166.v1

In that situation, CAR-T cells could not expand in-vivo and did not control the disease anymore, and the tumour continued growing after the treatment infusion.

The threshold of α_1 below which the tumour dynamics was controlled by the treatment was also found to be dependent on the value of the saturation parameter g_C as shown in Figure 2.

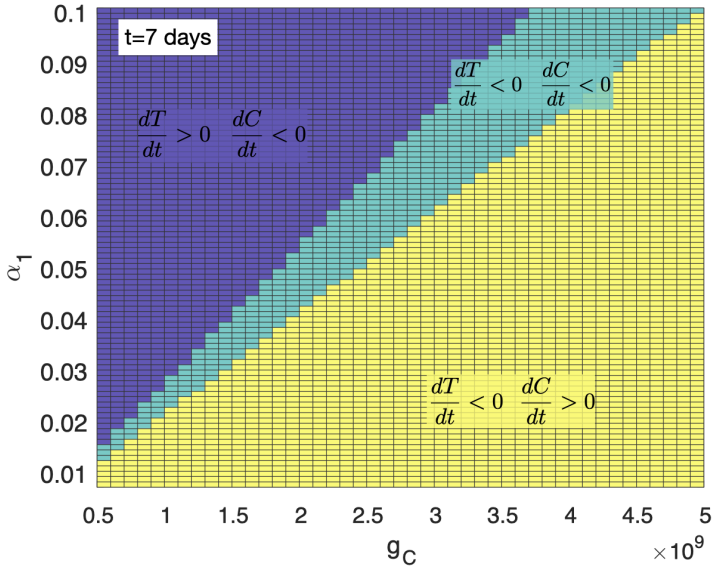

Figure 2. Parameter regions of control of the tumour growth dynamics seven days after infusion as a function of α_1 and g_C. Yellow areas show the parameter areas in which $dT/dt < 0, dC/dt > 0$, i.e. tumour was reducing its size and the CAR-T cell population increasing after seven days. Green areas are those in which $dT/dt < 0, dC/dt < 0$ after seven days, thus tumour mass was reducing its size but the CAR-T cell was being destroyed by the cancer cells immune suppression corresponding to transient effect of the therapy. Purple regions are those in which $dT/dt > 0, dC/dt < 0$. Thus, tumour was increasing its size and the CAR-T cell population decreasing after seven days, pointing out to therapy failure. Initial data used in the simulations were $C_0 = 8 \times 10^7$, $T_0 = 3.35 \times 10^{10}$ and parameter values $\tau_C = 7$ days, $\rho_C = 0.9$ day^{-1}, $\rho_T = 1/50$ day^{-1}, $\alpha_2 = 2.5 \times 10^{-10}$ day^{-1} cell^{-1}, $g_T = 10^{10}$.

3.2. Initial number of CAR-T cells injected affects the outcome of the therapy in model (1)

Next, we studied the effect of the number of CAR-T cells initially injected on the system's dynamics for the case of CAR-T cells targetting only the on-tumour antigen. To do so, we performed an extensive number of simulations of Eqs. (1) over the biologically feasible range of parameters. We found a dependence of the dynamics on the number of injected CAR-T cells. Results shown in Figure 3 present some examples for numbers of cells initially injected ranging from 5×10^7 to 1.5×10^8 cells.

There were two different types of dynamics in the tumour response depending on the initial choice of C_0. For the parameters listed in Fig. 3, there was a qualitative change of the dynamics around $C_0 = 2 \times 10^8$ cells. Thus, small doses of CAR-T cells led only to a small reduction in the tumour load (Figure 3(a)), while for doses larger than the mentioned threshold, the therapy was able to control tumour growth in-silico (see Figure 3(b)). The threshold was found to be related to the particular choice of parameter values and would change under different conditions.

This dynamic differs from what happens in leukaemias in which the outcome does not depend on the number of cells injected [26]. This is mainly due to the immune suppression capabilities of solid tumours included in our model equations.

Preprints (www.preprints.org) | NOT PEER-REVIEWED | Posted: 7 December 2020 doi:10.20944/preprints202012.0166.v1

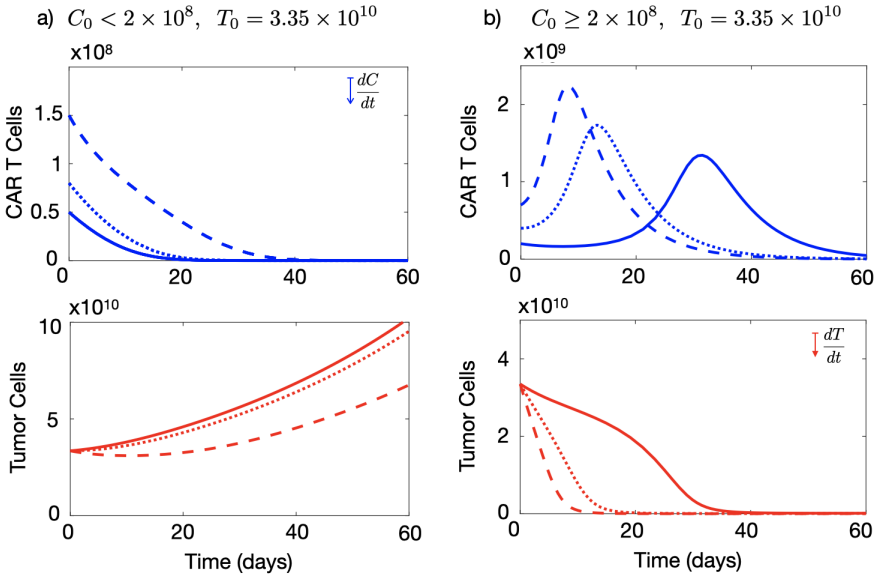

Figure 3. Injection of large numbers of CAR-T cells allows to overcome immune suppression effects of solid tumours in-silico. Longitudinal dynamics of the total number of CAR-T (blue) and tumour cells (red) ruled by Eq. (1). The curves correspond to different values of CAR-T cells injected in a patient bearing a number of $T_0 = 3.35 \times 10^{10}$ tumour cells. (a) CAR-T cell dynamics for $C_0 = 5 \times 10^7$ (solid line), $C_0 = 8 \times 10^7$ (dotted line), $C_0 = 1.5 \times 10^8$ (dashed line). (b) Longitudinal dynamics of the CAR-T cells for $C_0 = 2 \times 10^8$ (solid line), $C_0 = 4 \times 10^8$ (dotted line) and $C_0 = 7 \times 10^8$ (dashed line). The parameter values used in the simulations were $\tau_C = 7$ days, $\rho_C = 0.9$ day^{-1}, $\rho_T = 1/50$ day^{-1}, $\alpha_1 = 0.04$ day^{-1} cell^{-1}, $\alpha_2 = 2.5 \times 10^{-10}$ day^{-1} cell^{-1}, $g_T = 10^{10}$ and $g_C = 2 \times 10^9$.

3.3. Injection of a large number of CAR-T cells could allow for cure or prolonged tumour control in the presence of immune suppression

Next, we used the mathematical model as a tool to tackle the problem of tumour immunosuppression against CAR-T and explored different CAR-T cell treatment strategies in-silico. As a first test, we increased the dose of the CAR-T product with respect to the one used in Figure 3 to 4×10^8 cells injected. Figure 4(a) shows that in that situation and with a tumour immunosuppression rate of $\alpha_1 = 0.04$ day^{-1} it was possible to obtain a significant reduction in the number of tumour cells of more than four orders of magnitude lasting for six months that could be compatible either with cure or provide a window of opportunity for the application of other therapies.

However, the same figure shows that higher levels of immunosuppression ($\alpha_1 = 0.07$ day^{-1} and $\alpha_1 = 0.1$ day^{-1}) led to the failure of the therapy and a continuous increase in the population of cancerous cells. Higher doses of CAR T would have to be injected at these rates of immunosuppression to achieve control of the disease. Figure 4(c) shows that for $\alpha_1 = 0.1$ day^{-1} increasing the dose above 1.5×10^9 cells, led again to disease control.

This means that, even with immune suppression active, achieving very high levels of CAR-T cells could allow to overcome the tumour defenses and defeat the tumour. However, achieving such an initial high doses is practically unfeasible. We will discuss in Sec. 4 how to achieve those large CAR-T cell doses without having to infuse them externally.

3.4. A high initial tumour load favours CAR-T cell expansion

Surgical resection is performed regularly as an up-front therapy in different cancer types. For glioblastoma it is part of the standard treatment as it helps to rapidly reduce mass effect and neurologic symptoms. The initial tumour load on has a doubled-sided role. One side a high tumour load would favour the initial expansion of the CAR-T cells but on the other it may enhance tumour inmune

Preprints (www.preprints.org) | NOT PEER-REVIEWED | Posted: 7 December 2020 doi:10.20944/preprints202012.0166.v1

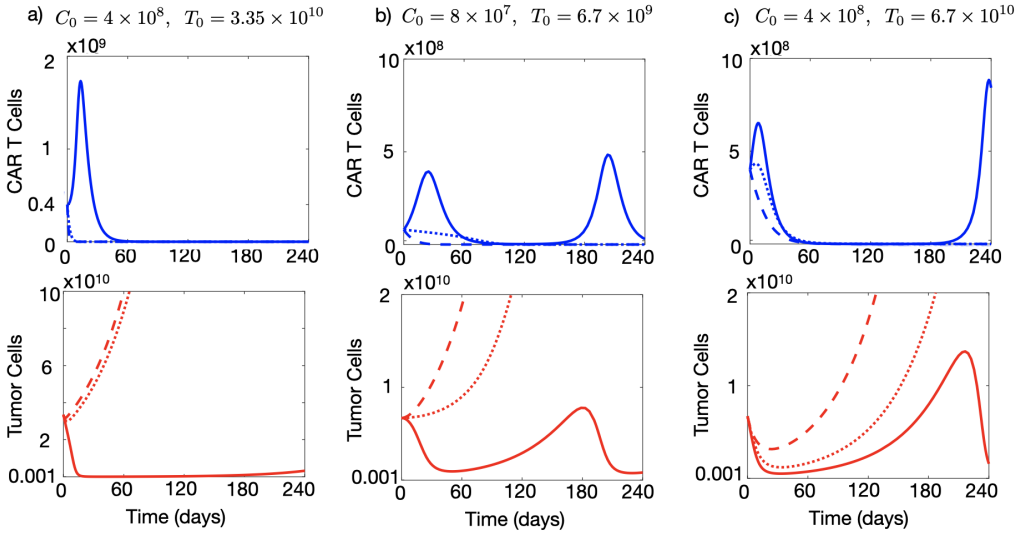

Figure 4. Simulated tumour and CAR T dynamics under different initial conditions for the number of injected cells and initial tumour load. Dynamics of the number of CAR-T cells (blue curves) and tumour cells (red curves) ruled by Eq. (1) in three different scenarios of immune suppression: $\alpha_1 = 0.04$ day^{-1}(solid lines), $\alpha_1 = 0.07$ day^{-1}(dotted lines) and $\alpha_1 = 0.1$ day^{-1}(dashed lines). Parameter values used in the simulations $\tau_C = 7$ days, $\rho_C = 0.9$ day^{-1}, $\rho_T = 1/50$ day^{-1}, $\alpha_2 = 2.5 \times 10^{-10}$ day^{-1} cell^{-1}, $g_T = 10^{10}$ and $g_C = 2 \times 10^9$.

suppression capabilities. Thus the question arises of what would be the optimal approach to use CAR-T cell treatments in combination with surgical resections.

To shed some light on the question we explored computationally the idea of using CAR-T cells after performing a partial surgical resection of the tumour, a frequent situation in the context of brain tumours. In that scenario one would start treatment with a hypothetical first-line therapy with CAR-T cells having a substantially smaller initial number of cancer cells. Assuming that the tumour load has been reduced to 20% of the initial one shown in Figure 4(a), Figure 4(b) shows the dynamics of CAR-T and tumour cells for $T_0 = 6.7 \times 10^9$ maintaining a low dose of CAR T, $C_0 = 8 \times 10^7$. The decrease in the initial tumour load led to a lower stimulation of the CAR-T cells and therapy failure even for tumours with low immune suppression capabilities ($\alpha_1 = 0.04$ day^{-1}). However, tumour relapses could be controlled by the CAR T cells in those tumours. Some additional tumour decrease was possible in the cases of greater immunosuppression ($\alpha_1 = 0.07$ day^{-1} and $\alpha_1 = 0.1$ day^{-1}) by increasing the initial CAR-T cell dose, as Figure 1(c) shows. In that case transient tumour stabilization was achieved lasting for several weeks although the final outcome was the same as in Figure 4(a).

4. Results (II): Therapy outcomes under tumour immune suppression using CAR-T cells with dual CAR groups with on- and off-tumour activity.

4.1. CAR-T cells with two targets provided long-time tumour control advantages in-silico.

We performed long-term simulations of Eqs. (1) with parameters as in Figure 4(a) and $\alpha_1 = 0.04$ day^{-1}, corresponding to weak immunosuppression. In this case, we observed the relapse of the disease in silico (see Figure 5(a)) around eight months after infusion. Tumour growth continued for several months leading to disease progression while CAR-T cells were exhausted approximately 4 months before relapse.

However, when repeating the same simulation using model Eqs. (2), i.e. in the case of using the CAR-T cells with two targets, we observed a substantially improved disease control in-silico. Results are summarized in Figure 5(b). The interaction between the CAR T cells in peripheral blood and the B cells stimulated the proliferation of the CAR-T cells and lead to an increased flow of these cells towards

Preprints (www.preprints.org) | NOT PEER-REVIEWED | Posted: 7 December 2020 doi:10.20944/preprints202012.0166.v1

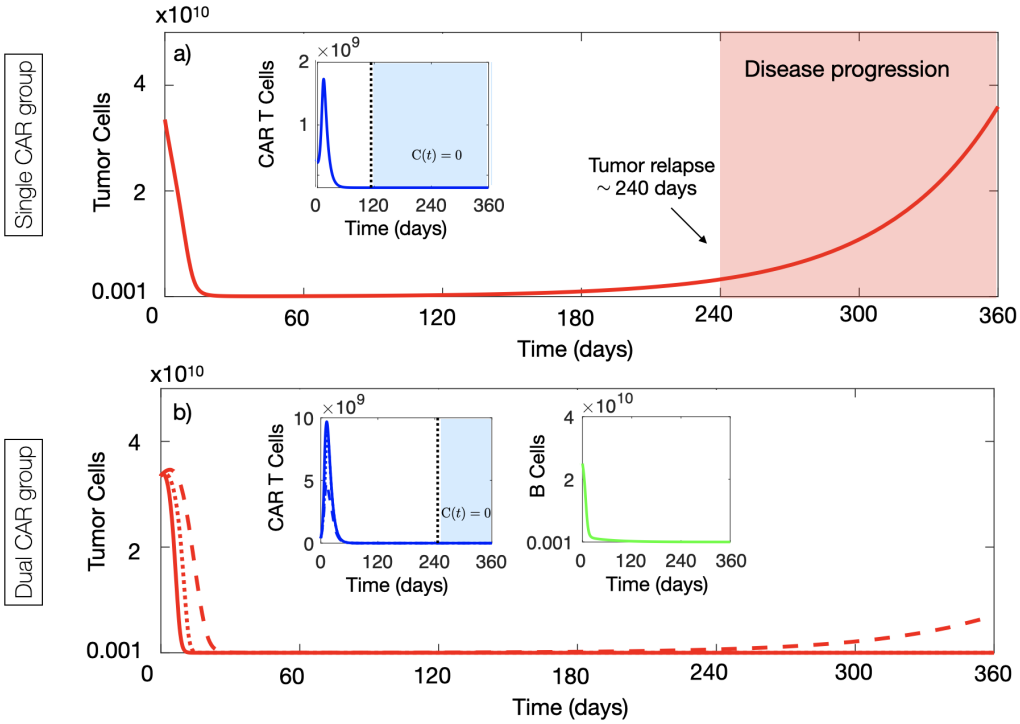

Figure 5. Long-term dynamics of virtual patients. a) Dynamics of the number of CAR-T (blue curve) and tumour cells (red curve) ruled by Eq. (1). Initial conditions and tumour inactivation rate used in the simulation were $C_0 = 4 \times 10^8$, $T_0 = 3.35 \times 10^{10}$ and $\alpha_1 = 0.01$ day^{-1}. b) Dynamics of the number of CAR-T cells (blue curves), B cells (green curve) and tumour cells (red curve) ruled by Eq. (2) in three different scenarios of immune suppression: $\alpha_1 = 0.04$ day^{-1}(solid lines), $\alpha_1 = 0.07$ day^{-1}(dotted lines) and $\alpha_1 = 0.2$ day^{-1} (dashed lines). Initial conditions used in the simulation were $\bar{C}_0 = 2 \times 10^8$, $C_0 = 0$, $B_0 = 2.5 \times 10^{10}$ and $T_0 = 3.35 \times 10^{10}$ cells. Parameter values used in the simulations were $\tau_C = 7$ days, $\rho_{\bar{C}} = \rho_C = 0.9$ day^{-1} , $\rho_T = 1/50$ day^{-1}, $\alpha_2 = 2.5 \times 10^{-10}$ day^{-1} cell^{-1}, $g_T = 10^{10}$ cells, $g_C = 2 \times 10^9$ cells, $g_B = 10^{10}$ cells, $k = 0.2$, $\alpha_B = 4.5 \times 10^{-11}$ day^{-1} cell^{-1} and $\tau_B = 60$ day^{-1}.

the tumour. In this case, we observe an improved expansion of the initial CAR-T cells delivered and persistence of the CAR-T product in the tumour tissue for longer times. Thus, by overcoming the tumour immunosuppressive environment, the proposed use of dual CAR-Ts could lead to improved tumour control. Figure 5(b) also shows the results when applying dual CAR T therapy in more immunosuppressive tumours, where single-target therapy would have failed. Thus, the use of dual target CAR-T with on- and off-tumour activity showed a substantially improved anti-tumour activity in comparison with the single-target CARs.

4.2. Dual CAR-T improves the possibility of therapy success

Finally, we performed a systematic study of the possibility of controlling tumour growth using the single and double CAR-T therapies. Figure 6 shows the results for different values of the tumour immunosuppression strength as a function of the initial number of CAR-T and tumour cells. Tumour was considered to be controlled if after six months, the number of tumour cells was below 10% of its peak value. A threshold effect was clearly observed, with tumour control at six months being a function of α_1, C_0, and T_0. The best results were obtained for double CAR T-cell therapy, which was capable of controlling a substantially larger number of tumours according to their size and immunosuppressive capacity, with lower doses of the CAR-T product (see Figure 6(d-f)). For the same value of α_1 (compare Figs. 6(c) and (d)), dual-CAR was substantially more effective in achieving tumour control. Moreover, in situations with small initial tumour cell loads, the dual-CAR treatment was effective even for large

Preprints (www.preprints.org) | NOT PEER-REVIEWED | Posted: 7 December 2020 doi:10.20944/preprints202012.0166.v1

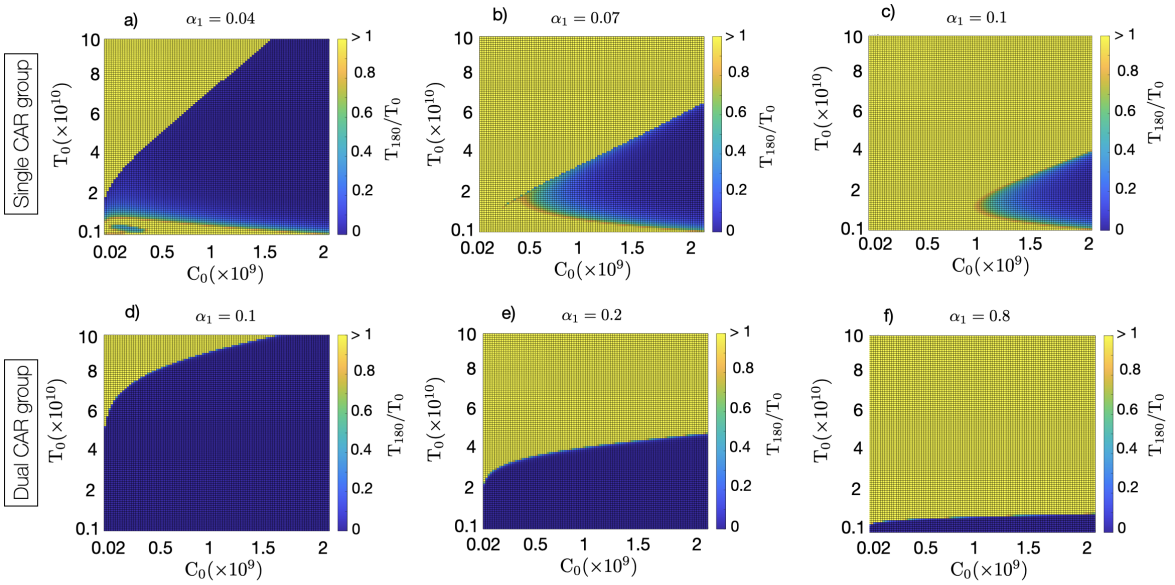

Figure 6. Colormap plots of the percentage of change in tumour load at six months compared to the initial load measured by the fraction $T(180)/T_0$, as a function of the initial number of CAR-T and tumour cells, over three immunosuppression scenarios: (a) $\alpha_1 = 0.04$ day^{-1} , (b) $\alpha_1 = 0.07$ day^{-1}, (c,d) $\alpha_1 = 0.1$ day^{-1}, (e) $\alpha_1 = 0.2$ day^{-1} and (f) $\alpha_1 = 0.8$ day^{-1}. Blue areas show the initial configurations of injected CAR-T cells (C_0) and tumour loads (T_0) leading to tumour control after six months. Subplots (a-c) show the results obtained using a single CAR as ruled by Eqs. (1). Subplots (d-f) shows results of computer simulations with the dual CARs obtained using Eqs. (2). Parameter values used in the simulations were $\tau_C = 7$ days, $\rho_{\bar{C}} = \rho_C = 0.9$ day^{-1} , $\rho_T = 1/50$ day^{-1}, $\alpha_2 = 2.5 \times 10^{-10}$ day^{-1} cell^{-1}, $g_T = 10^{10}$, $g_C = 2 \times 10^9$, $g_B = 10^{10}$, $k = 0.2$, $\alpha_B = 4.5 \times 10^{-11}$ day^{-1} cell^{-1} and $\tau_B = 60$ day^{-1}.

values of the tumour immune suppression parameter, what points out to a potential success of the therapy when using the treatment early after surgery.

5. Discussion

After their success in treating different haematological cancers, CAR-T cell treatments have become one of the most promising novel immunotherapies in cancer. However, the translation of their therapeutical benefits to solid tumours faces significant challenges, one of them being the immunosuppressive capabilities of the tumour microenvironment and more specifically of tumour cells.

The simulations of our mathematical model point out that the injection of a massive amount of CAR-T cells could be able to overcome the inmune suppression tumour capabilities. The idea is simple: just trow in many more T cells than the tumour can deactivate. However, this is not currently possible technically with current CAR-T products, since the number of T-cells that can be obtained currently are orders of magnitude below the threshold for such an assault on the tumour to succeed. Moreover only a fraction of the cells injected in the blood stream traffics to the tumour site. Although this can be partially overcome by the direct delivery of the CAR-T cells to the tumour sites these ideas have not lead to sustained therapeutical success when treating glioblastomas.

Thus, one alternative option is to generate an army of CAR-T cells within the body. For that purpouse, any target allowing for the expansion of the T cells without a significant toxicity could be used. This lead us to the idea that dual-target CAR-T cells, one with on-tumour activity and other with off-tumour activity on a large population of non-essential healthy cells whose elimination does not threaten patient survival. One example of such target could be CD19 because of the large number

 doi:10.20944/preprints202012.0166.v1

of B-cells present in the organism, the fact that CD19 is not expressed in other tissues, and that the toxicity of current CAR-T products targetting CD19 is now well controlled.

Interestingly, our mathematical model captured the difficulties for CAR-T cell expansion when tumour immune suppression was accounted for. As in different clinical studies, the model showed that CAR-T cells targeting solid tumours have poor persistence properties, even with high doses of CAR-T delivered. Simulations recapitulated the relevance of the dose injected for the early outcome of the therapy. The exact dose threshold value that can be effective in the tumour control would depend on the its characteristics, and would be patient- and tumour- dependent. Immunosuppressive tumours such as glioblastoma may require higher doses of injected CAR-T cells to achieve a significant reduction in the tumour load. However, even in poorly immunosuppressive environments, the escape of tumour due to the limiting effect of the immunosuppression was found to be enough to allow for relapse in the medium term.

We also explored in-silico the idea of treating resected tumours with the single-CAR T cells, i.e. in scenarios of a reduction of the initial tumour load. In that case, a modest expansion of CAR-T cells was observed due to the lower levels of tumour targets. In principle, the reduction in tumour size could help in limiting the effect of tumour immunosuppression. We found in-silico that both processes overlapped leading to an initial reduction in tumour size, but eventually the tumour grew back. Better results were obtained in-silico for long-term tumour control when a high dose of CAR T cells was administered to a large initial tumour. The problem is that, taking into account the reduction of cells from the injected ones to those trafficking to the tumour region, too high amounts of CAR-T cells would be necessary, what would be technically unfeasible.

The CAR-T with dual CAR groups targetting CD19 and the tumour antigen, would promote further stimulation of CAR-T cells through their interaction with B cells, providing a powerful source of tumour-targetting CAR-T cells. In fact, interaction with B cells is likely to occur early as they are found in blood and lymphoid organs [48]. Normal B cells would then provide a non-tumour dependent, self-renewing antigen source to support CAR-T. This double targeting on and off the tumour would provide a simple and pragmatic solution to improve the problem of trafficking and CAR-T cell deactivation due to immune suppression by tumour cells.

Our simple simulation model of this scenario provided substantial tumour control advantages in-silico over the single-CAR situation. Substantial improvements in effectiveness were observed in cases in which CAR-T cells with a single on-tumour target had difficultities in controlling the tumour. The first situation was highly immunosuppressive tumours, were therapy success was substantially improved by the initial boost in anti-tumour cells generated by the substantially larger initial expansion. The second situation was the one of small initial tumour loads, in which single-target CAR-T expansion would be less likely to be substantial, e.g. in cases in which an initial surgery had left only a remnant of infiltrative tumour cells. In that case, the major contribution to CAR-T cell expansion came from the CD19-bearing cells and led to the success of dual CAR therapy in silico.

The fact that tumour control was substantially improved using the dual CARs for low initial tumour loads is reasonable since the CARs will be expanded off-tumour and the immune suppression capabilities of the tumour would be smaller. This means that an optimal use of this therapy would be to use it right away after surgical resection for patients having a macroscopically complete resection. Those patients have both a low initial tumour load and have mostly a remnant of tumour cells that would be infiltrating the normal brain parenchyma thus in areas were vasculature would be normal and accessible to circulating CAR-T cells.

The proposed strategy has the only limitation of the toxicity of the treatment on $CD19^{+}$ cells. Acute toxicity is mostly related to the cytokine release syndrome and neurotoxicity. These side effects of the treatment can be life-threatening in a subset of patients. However, tocilizumab and corticosteroids have been used to manage these toxicities, enabling CD19 CAR-T cells to be administered without obvious compromise in efficacy [49,50].

 doi:10.20944/preprints202012.0166.v1

The PD-1/PD-L1 interaction of T cells and tumour cells leads to the inhibition of the effector function of T cells, therefore blocking this interaction has the potential to significantly enhance the anti-tumour activity of T cells and reducing T cell exhaustion. The combination of CAR-T with PD-1 blockade, in our case leading to reduction in the immune suppression parameter α_1, is a promising strategy to enhance the effectiveness of CAR-T cells therapies [47].

Thus, our study suggests an optimal protocol for the optimal use of these dual-target CAR-Ts with on- and off-tumour activity. Patient blood samples should be taken before surgery in order to start with the preparation and in-vitro expansion of the CAR-T product and the patient should receive surgery in the meantime and allow for a recovery time. After that the dual CAR-Ts should be infused, may be in combination with anti-PD1 treatment, and finally cytotoxic therapies (radiation therapy and chemotherapy) could be also applied to kill potentially resistant cells not bearing the CAR-T tumour target.

6. Conclusions

In summary, we have constructed a mathematical model of a solid tumour response to CAR-T cells with dual targets: one of them recognizing a tumour antigen and the other recognizing an off-tumour antigen present in normal cells such as $CD19^+$ B-cells. When only the tumour antigen was present, the therapy could overcome the tumour immune suppression only when unrealistically large numbers of CAR-T cells were injected. The use of dual CARs let the expansion of the CAR-T population to happen even in the presence of immune suppression exerted by tumour cells on the T-cells and allowing to reach appropriate therapeutic levels of the T-cell population. In our simulations, that resulted in long-term tumour control what would provide an additional tool in the fight against aggressive cancers with few therapeutic options such as glioblastoma. We also found in-silico that an optimal use of the dual-CAR-T cell therapy for glioblastoma would be to inject them right after extensive surgical resections and before the use of cytotoxic treatments.

In this paper we intended only to provide a theoretical proof of concept of the phenomenon. There is much work to do to explore mathematically the dynamical interplay of the different biological processes, and to find the parameter ranges best describing these phenomena. We hope that this work will stimulate the development of experimental studies, testing the potential effectiveness of the concepts proposed here. If successful, CAR-T with dual targets could become a novel ingredient in combination therapies against aggressive solid tumours such as glioblastoma.

Author Contributions: Conceptualization, V.M.P-G., M.R-O., A. P-M.; methodology, O.L-T. and V.M.P-G.; investigation, O.L-T.; resources, V.M.P-G.; writing–original draft preparation, O.L-T. and V.M.P-G.; writing–review and editing, M.R-O., A. P-M.; visualization, O.L-T.; supervision, V.M.P-G.; project administration, V.M.P-G..; funding acquisition, V.M.P-G. All authors have read and agreed to the published version of the manuscript.

Funding: This work has been funded by James S. Mc. Donnell Foundation (USA) 21st Century Science Initiative in Mathematical and Complex Systems Approaches for Brain Cancer (Collaborative award 220020450), Ministerio de Ciencia e Innovación, Spain (grant number PID2019-110895RB-I00), and Junta de Comunidades de Castilla-La Mancha (grant number SBPLY/17/180501/000154). OLT is supported by a PhD Fellowship from the University of Castilla-La Mancha research plan.

Acknowledgments: We would like to acknowledge Álvaro Martínez-Rubio, Salvador Chulián and María Rosa (Department of Mathematics, Universidad de Cádiz, Puerto Real, Cádiz, Spain) for discussions on CAR T cell modelling.

Conflicts of Interest: The authors declare no conflict of interest.

Abbreviations

CAR	Chimeric antigen receptor
GBM	Glioblastoma

Preprints (www.preprints.org) | NOT PEER-REVIEWED | Posted: 7 December 2020 doi:10.20944/preprints202012.0166.v1

Appendix A. Basic properties of the mathematical model Eqs. (1)

Theorem 1. *For any non negative initial data (C_0, T_0) and all the parameters of the model being positive, the solutions to Eqs. (1) exist for $t > 0$, are non negative and unique.*

Proof. The ODE system (1) has bounded coefficients and the right hand side of the system is a continuous function of (C, T) in the domain $R^2_{+,0}$, thus the local existence of solutions follows from classical ODE theory. Since the partial derivatives of the velocity field are continuous and bounded, uniqueness follows from the Picard-Lindelof theorem.

Let us rewrite Eqs. (1) when $g = 0$ as

$$\dot{C} = \left[\frac{\rho_C T}{g_T + T} - \frac{\alpha_1 T}{g_C + C} - 1/\tau_C\right] C, \tag{A1a}$$

$$\dot{T} = (\rho_T - \alpha_2 C)\, T, \tag{A1b}$$

then we may write

$$C(t) = C_0 \exp\left(\int_{t_0}^{t} \left[\frac{\rho_C T(t')}{g_T + T(t')} - \frac{\alpha_1 T(t')}{g_C + C(t')} - \frac{1}{\tau_C}\right] dt'\right), \tag{A2a}$$

$$T(t) = T_0 \exp\left(\int_{t_0}^{t} \left(\rho_T - \alpha_2 C(t')\right) dt'\right), \tag{A2b}$$

what leads to the positivity of solutions. □

Appendix A.1. Equilibria of the model Eqs. (1) and local stability analysis

The equilibria of Eqs. (1) are given by the equations

$$0 = \left[\frac{\rho_C T}{g_T + T} - \frac{\alpha_1 T}{g_C + C} - 1/\tau_C\right] C, \tag{A3a}$$

$$0 = [\rho_T - \alpha_2 C]\, T, \tag{A3b}$$

Eq. (A3b) leads to either $T = 0$ or $C = \rho_T/\alpha_2$. Using $T = 0$ and Eq. (A3a) we obtain $C = 0$. Then using $C = \rho_T/\alpha_2$ and Eq. (A3a) allows us to obtain the quadratic expressions for T,

$$\alpha T^2 + T(\alpha g_T - \rho_C + 1/\tau_C) + g_T/\tau_C = 0, \tag{A4}$$

where $\alpha = \frac{\alpha_1}{g_C + \rho_T/\alpha_2}$. The solutions of Eq. (A4) are

$$T^*_{1,2} = \frac{-(\alpha g_T - \rho_C + 1/\tau_C) \pm \sqrt{(\alpha g_T - \rho_C + 1/\tau_C)^2 - 4\alpha g_T/\tau_C}}{2\alpha g_T}, \tag{A5}$$

where the discriminant is non negative and the solutions are positive in the cases: *i)* $\rho_C \geq (\sqrt{\alpha g_T} + \sqrt{1/\tau_C})^2$ and *ii)* $\rho_C < (\sqrt{\alpha g_T} - \sqrt{1/\tau_C})^2$ and $\rho_C < \alpha g_T$.

The equilibrium points of the system under these conditions are

$$E_1 = (0, 0), \tag{A6a}$$

$$E_{2,3} = (\frac{\rho_T}{\alpha_2}, T^*_{1,2}). \tag{A6b}$$

In the particular case $\rho_C = (\sqrt{\alpha g_T} + \sqrt{1/\tau_C})^2$, there are only two equilibria since $E_2 = E_3 = (\frac{\rho_T}{\alpha_2}, \frac{1}{\sqrt{\alpha g_T \tau_C}})$.

Preprints (www.preprints.org) | NOT PEER-REVIEWED | Posted: 7 December 2020 doi:10.20944/preprints202012.0166.v1

The Jacobian of the differential equations (1) is

$$J = \begin{pmatrix} \frac{\rho_C T}{g_T+T} - 1/\tau_C - \frac{\alpha_1 TC}{(g_C+C)^2} & \frac{\rho_C g_T C}{(g_T+T)^2} - \frac{\alpha_1 C}{g_C+C} \\ -\alpha_2 T & \rho_T - \alpha_2 C \end{pmatrix}. \tag{A7}$$

Let us now use Eq. (A7) to study the local stability of the different equilibria given by Eqs. (A6). First, for E_1 we get

$$J(E_1) = \begin{pmatrix} -1/\tau_C & 0 \\ 0 & \rho_T \end{pmatrix}. \tag{A8}$$

The eigenvalues of $J(E_1)$ are

$$\lambda_1 = -1/\tau_C, \lambda_2 = \rho_T, \tag{A9}$$

thus the equilibrium point E_1 is unstable. For the second equilibrium point an analytical expression cannot be obtained for the eigenvalues, therefore carrying out a stability study for this point is very complex. Therefore, we carry out a study of the dynamics of the system for a better understanding of the system (1).

Appendix A.2. Dynamical system analysis of the model Eqs. (1)

The dynamics of the system may be represented as trajectories in a two-dimensional phase-space of cancer cells and CAR T cells. Figure A1 shows the trajectories for differents initial conditions.

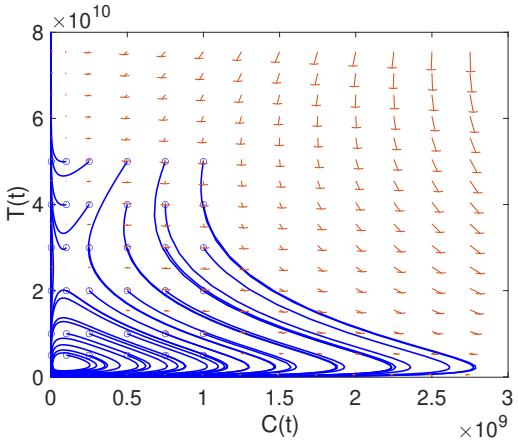

Figure A1. Phase space of model equations (1). Some dynamics are represented as trajectories in the two-dimensional space (C(t),T(t)) (CAR T-cells, tumour cells) for default parameter values $\tau_C = 7$ days, $\rho_C = 0.9$ day^{-1}, $\rho_T = 1/50$ day^{-1}, $\alpha_1 = 0.04$ day^{-1} cell^{-1}, $\alpha_2 = 2.5 \times 10^{-10}$ day^{-1} cell^{-1}, $g_T = 10^{10}$ and $g_C = 2 \times 10^9$.

Appendix B. Basic properties of Eqs. (2)

Theorem 2. *For any non negative initial data $(\bar{C}_0, B_0, C_0, T_0)$ and all the parameters of the model being positive, the solutions to Eqs. (2) exist for $t > 0$, are non negative and unique.*

Proof. We analyze the behavior of the vector field to prove the non-negativity of the solutions. Let $F = F(x) = \frac{dx}{dt}$ be the vector field of the system (2) with solucions $x = (\bar{C}(t), B(t), C(t), T(t))$. Starting from the positive initial condition $(\bar{C}_0, B_0, C_0, T_0)$, we study the direction of the vector field F at hyper-surfaces $\bar{C} = 0$, $B = 0$, $C = 0$ and $T = 0$. Let us denote n_i to the normal unit vector in the negative direction to plane $x_i = 0$, for $i = 1, 2, 3, 4$ (i.e, $n_1 = (-1, 0, 0, 0)$, $n_2 = (0, -1, 0, 0)$, ..., $n_4 = (0, 0, 0, -1)$) and let consider the scalar products $F \cdot n_i$. Then, $F \cdot n_1 = 0$, $F \cdot n_2 = 0$ and $F \cdot n_4 = 0$ at hyper-surfaces $\bar{C} = 0$, $B = 0$ and $T = 0$, respectively. Then, the hyper-surfaces $\bar{C} = 0$, $B = 0$ and $T = 0$ are invariant. In the case of hyper-surface $C = 0$ it is obtained that $F \cdot n_3 = -k\bar{C} < 0$.

Preprints (www.preprints.org) | NOT PEER-REVIEWED | Posted: 7 December 2020 doi:10.20944/preprints202012.0166.v1

Hence, $R^4_{+,0}$ is a positive invariant domain for Eqs. (2). Therefore, we have prove the non-negativity of solutions $(\bar{C}(t), B(t), C(t), T(t))$.

Since the ODE system (2) has non-negative solutions and the right hand side of the system is a continuous function of $(\bar{C}, B, C, T)$ in the domain $R^4_{+,0}$, existence of solutions follows form the Cauchy-Peano theorem. Moreover, the partial derivatives of the velocity field are also continuous and bounded in $R^4_{+,0}$. Then, using the Picard-Lindelof theorem we have prove the uniqueness of solutions. □

Appendix B.1. Equilibria of the model Eqs. (2) and local stability analysis

We begin by calculating the fixed points and determine their stability. These are the points $E_1 = (0,0,0,0)$ and $E_2 = (0,0,\frac{\rho_T}{\alpha_2}, T^*_{1,2})$, where $T^*_{1,2}$. To analyze the stability of these points, we calculate the Jacobian matrix of Eqs.(2)

$$J = \begin{pmatrix} \frac{\rho_C B}{g_B+B} - 1/\tau_C - k & \frac{\rho_C \bar{C} g_B}{(g_B+B)^2} & 0 & 0 \\ -\alpha_B B & -\alpha_B \bar{C} - 1/\tau_B & 0 & 0 \\ k & 0 & \frac{\rho_C T}{g_T+T} - 1/\tau_C - \frac{\alpha_1 TC}{(g_C+C)^2} & \frac{\rho_C g_T C}{(g_T+T)^2} - \frac{\alpha_1 C}{g_C+C} \\ 0 & 0 & -\alpha_2 T & \rho_T - \alpha_2 C \end{pmatrix}.$$

For the equilibrium point $E_1 = (0,0,0,0)$, the Jacobian matrix is

$$J = \begin{pmatrix} -1/\tau_C - k & 0 & 0 & 0 \\ 0 & -1/\tau_B & 0 & 0 \\ k & 0 & -1/\tau_C & 0 \\ 0 & 0 & 0 & \rho_T \end{pmatrix}.$$

and the eigenvalues are $\lambda_1 = -(k + 1/\tau_C)$, $\lambda_2 = -1/\tau_B$, $\lambda_3 = -1/\tau_C$ and $\lambda_4 = \rho_T$. Thus, E_1 is an unstable equlibrium point. The study of the stability of E_2 is similar to its analogue in the case of Eqs. 1, where a simple analytical expression for the eigenvalues cannot be obtained.

References

1. Feins, S.; Kong, W.; Williams, E.F.; Milone, M.C.; Fraietta, J.A. An introduction to chimeric antigen receptor (CAR) T-cell immunotherapy for human cancer. *Am. J. Hematol.* **2019**, *94*, S3–S9. doi: 10.1002/ajh.25418. PMID: 30680780.
2. Maude, S.L.; Laetsch, T.W.; Buechner, J.; Rives, S.; Boyer, M.; et al. Tisagenlecleucel in children and young adults with B-cell lymphoblastic leukemia. *N. Engl. J. Med.* **2018**, *378(5)*, 439–448. doi: 10.1056/NEJMoa1709866. PMID: 29385370; PMCID: PMC5996391.
3. Pan, J.; Yang, J.F.; Deng, B.P.; Zhao, X.J.; Zhang, X.; Lin, Y.H., Wu, Y.N., Deng, Z.L., Zhang, Y.L., Liu, S.H., Wu, T., Lu, P.H., Lu, D.P., Chang, A.H., Tong, C.R. High efficacy and safety of low-dose CD19$^-$directed CAR-T cell therapy in 51 refractory or relapsed B acute lymphoblastic leukemia patients. *Leukemia*, **2017** *31(12)*, 2587–2593. doi: 10.1038/leu.2017.145. PMID: 28490811.
4. Miliotou, A.N.; Papadopoulou, L.C. CAR T-cell Therapy: A New Era in Cancer Immunotherapy. *Curr. Pharm. Biotechnol* **2018**, *19(1)*, 5–18. doi:10.2174/1389201019666180418095526. PMID: 29667553.
5. D'Agostino, M.; Raje, N. Anti-BCMA CAR T-cell therapy in multiple myeloma: can we do better? *Leukemia*, **2020**, *34(1)*, 21–34. doi: 10.1038/s41375-019-0669-4. PMID: 31780814.
6. Chavez, J. C.; Bachmeier, C.; Kharfan-Dabaja, M. A. CAR T-cell therapy for B-cell lymphomas: clinical trial results of available products *Ther Adv Hematol.*, **2019**, *10*, 2040620719841581. doi: 10.1177/2040620719841581. PMID: 31019670; PMCID: PMC6466472.
7. Wang, QS.; Wang Y.; Lv, HY.; Han, QW.; Fan, H.; Guo, B.; Wang, LL.; Han, WD. Treatment of CD33-directed chimeric antigen receptor-modified T cells in one patient with relapsed and refractory acute myeloid leukemia. *Molecular Therapy*, **2015**, *23(1)*, 184-191. doi: 10.1038/mt.2014.164. PMID: 25174587; PMCID: PMC4426796.

8. Martínez, M.; Moon, E.K. CAR T Cells for Solid Tumors: New Strategies for Finding, Infiltrating, and Surviving in the Tumor Microenvironment. *Front. Immunol.* **2019**, *10*, 128. doi: 10.3389/fimmu.2019.00128. PMID: 30804938; PMCID: PMC6370640.
9. Bagley, S. J.; O'Rourke, D. M. Clinical investigation of CAR T cells for solid tumors: Lessons learned and future directions. *Pharmacology &Therapeutics* **2020**, *205*, 107419. doi: 10.1016/j.pharmthera.2019.107419. PMID: 31629009.
10. Castellarin, M.; Watanabe, K.; June, C.H.; Kloss, C.C.; Posey Jr, A.D. Driving CARs to the clinic for solid tumors. *Gene Therapy*. **2018**, *25*, 165–175. https://doi.org/10.1038/s41434-018-0007-x
11. Hege, KM.; Bergsland, EK.; Fisher, GA.; Nemunaitis, JJ.; Warren, RS.; McArthur, JG.; Lin, AA.; Schlom, J.; June, CH.; Sherwin, SA. Safety, tumor trafficking and immunogenicity of chimeric antigen receptor (CAR)-T cells specific for TAG-72 in colorectal cancer. *J Immunother Cancer*. **2017**, *21*, 5–22. doi: 10.1186/s40425-017-0222-9. PMID: 28344808; PMCID: PMC5360066.
12. Ma, S.; Li, X.; Wang, X.; Cheng, L.; Li, Z.; Zhang, C.; Ye, Z.; Qian, Q. Current Progress in CAR-T Cell Therapy for Solid Tumors. *Int. J. Biol. Sci.* **2019** *15(12)*, 2548–2560. doi: 10.7150/ijbs.34213. PMID: 31754328; PMCID: PMC6854376.
13. Hong, M.; Clubb, JD.; Chen, YY. Engineering CAR-T Cells for Next-Generation Cancer Therapy *Cancer Cell*. **2020** *38(4)*, 473–488. doi: 10.1016/j.ccell.2020.07.005. PMID: 32735779.
14. Han, X.; Wang, Y.; Wei, J.; Han, W. Multi-antigen-targeted chimeric antigen receptor T cells for cancer therapy. *Journal of Hematology & Oncology*. **2019**, *12(1)*, 128. doi: 10.1186/s13045-019-0813-7. PMID: 31783889; PMCID: PMC6884912.
15. Rafiq, S.; Hackett, CS.; Brentjens, RJ. Engineering strategies to overcome the current roadblocks in CAR T cell therapy. *Nature Reviews Clinical Oncology volume*. **2020**, *17(3)*, 147–167. doi: 10.1038/s41571-019-0297-y. PMID: 31848460; PMCID: PMC7223338.
16. Hegde, M.; Corder, A.; Chow, K.K.H.; Mukherjee, M.; Ashoori, A.; et al. Combinational Targeting Offsets Antigen Escape and Enhances Effector Functions of Adoptively Transferred T Cells in Glioblastoma. *Molecular Therapy*. **2013**, *21(11)*, 2087–2101. https://doi.org/10.1038/mt.2013.185
17. Roybal, K.T.; Rupp, L.J.; Morsut, L.; Walker, W.J.; McNally, K.A.; Park, J.S.; LimPrecision, W.A. Precision Tumor Recognition by T Cells With Combinatorial Antigen-Sensing Circuits. *Cell*. **2016**, *164(4)*, 770–779. doi: 10.1016/j.cell.2016.01.011. PMID: 26830879; PMCID: PMC4752902.
18. Feng, KC.; Guo, YL.; Liu, Y.; Dai, HR.; Wang, Y.; Lv, HY.; Huang, JH.; Yang, QM.; Han, WD. Cocktail treatment with EGFR-specific and CD133-specific chimeric antigen receptor-modified T cells in a patient with advanced cholangiocarcinoma *Journal of Hematology & Oncology*. **2017**, *10(1)*, 4. doi: 10.1186/s13045-016-0378-7. PMID: 28057014; PMCID: PMC5217546.
19. Altrock, P.M.; Liu, L.L., Michor, F. The mathematics of cancer: Integrating quantitative models. *Nature Reviews Cancer*. **2016**, *15*, 730–745. doi: 10.1038/nrc4029. PMID: 26597528.
20. Pérez-García, V.M.; et al. Applied mathematics and nonlinear sciences in the war on cancer. *Appl. Math. Nonlin. Sci.* **2016** *1(2)*, 423-436.
21. Sahoo, P.; Yang, X.; Abler, D.; Maestrini, D.; Adhikarla, V.; Frankhouser, D.; Cho, H.; Machuca, V.; Wang, D.; Barish, M.; Gutova, M.; Branciamore, S.; Brown, C.E.; Rockne, R.C. Mathematical deconvolution of CAR T-cell proliferation and exhaustion from real-time killing assay data. *J. R. Soc. Interface* **2020**, *17*, 20190734.
22. Baar, M.; Coquille, L.; Mayer, H.; Holzel, M.; Rogava, M.; Tuting, T.; Bovier, A. A stochastic model for immunotherapy of cancer. *Sci. Rep.* **2016**, *6*, 24169. https://doi.org/10.1038/srep24169
23. Kimmel, G.J.; Locke, F.L.; Altrock, P.M. (2019) Evolutionary Dynamics of CAR T Cell Therapy. *bioRxiv* 717074.
24. Rodrigues, B.J.; Carvalho Barros, L.R.; Almeida, R.C. (2019) Three-Compartment Model of CAR T-cell Immunotherapy. *bioRxiv* 779793
25. Mostolizadeh, R.; Afsharnezhad, Z.; Marciniak-Czochra, A. Mathematical model of Chimeric Anti-gene Receptor (CAR) T cell therapy with presence of cytokine. *Numerical Algebra Control & Optimization* **2018**, *8(1)*, 63–80
26. León-Triana, O.; Soukaina, S.; Calvo, G.F.; Belmonte-Beitia, J.; Chulián, S.; Martínez-Rubio, A.; Rosa, M.; Pérez-Martínez, A.; Ramírez-Orellana, M.; Pérez-García, V.M. CAR T cell therapy in B-cell acute lymphoblastic leukaemia: Insights from mathematical models, *Communications in Nonlinear Science and Numerical Simulation* **2021**, *94*, 105570.

27. Pérez-García V.M.; León-Triana, O.; Rosa, M.; Pérez-Martínez, A.; Ramírez-Orellana, M.; Pérez-García, V.M. (2020) CAR T cells for T-cell leukemias: Insights from mathematical models. *Communications in Nonlinear Science and Numerical Simulation* **2021**, *94*.
28. Chulián, S.; Martínez-Rubio, A.; Rosa, M.; Pérez-García, V. M. (2021) Mathematical models of Leukaemia and its treatment: A review. *SEMA Journal* **2021**.
29. Brown, M. P.; Ebert, L. M.; Gargett, T. Clinical chimeric antigen receptor-T cell therapy: a new and promising treatment modality for glioblastoma. *Clinical & Translational Immunology* **2019**, *8(5)*, e1050. doi: 10.1002/cti2.1050. PMID: 31139410; PMCID: PMC6526894.
30. Bagley, S.J.; Desai, A. S.; Linette, G.P.; June, C. H.; O'Rourke, D. M. CAR T-cell therapy for glioblastoma: recent clinical advances and future challenges. *Neuro-Oncology* **2018**, *20(11)*, 429–1438. doi: 10.1093/neuonc/noy032. PMID: 29509936; PMCID: PMC6176794.
31. Brown, C.E.; Alizadeh, D.; Starr, R.; et al. Regression of glioblastoma after chimeric antigen receptor T-cell therapy. *N Engl J Med.* **2016**, *375(26)*, 2561–2569. doi: 10.1056/NEJMoa1610497. PMID: 28029927; PMCID: PMC5390684.
32. Brown, C.E.; Badie, B.; Barish, M.E.; Weng, L.; Ostberg, J.R.; Chang, W.C.; et al. Bioactivity and safety of IL13Rα2- redirected chimeric antigen receptor CD8+ T cells in patients with recurrent glioblastoma. *Clin. Cancer Res.* **2015**, *21(18)*, 4062–4072. doi: 10.1158/1078-0432.CCR-15-0428. PMID: 26059190; PMCID: PMC4632968.
33. O'Rourke, D.M.; Nasrallah, M.P.; Desai, A.; et al. A single dose of peripherally infused EGFRvIII-directed CAR T cells mediates antigen loss and induces adaptive resistance in patients with recurrent glioblastoma. *Sci. Transl. Med.* **2017**, *9(3999)*, eaaa0984. doi: 10.1126/scitranslmed.aaa0984. PMID: 28724573; PMCID: PMC5762203.
34. Mahlbacher, G. E.; Reihmer, K. C.; Frieboes H. B. Mathematical modeling of tumor-immune cell interactions. *Journal of Theoretical Biology* **2019**, *469*, 47–60. doi: 10.1016/j.jtbi.2019.03.002. PMID: 30836073; PMCID: PMC6579737.
35. Brown, C.E.; Aguilar, B.; Starr, R., et al. Optimization of IL13Ra2-targeted chimeric antigen receptor T cells for improved anti-tumor efficacy against glioblastoma. *Molecular Therapy* **2018**, *26(1)*, 31–44. doi: 10.1016/j.ymthe.2017.10.002. PMID: 29103912; PMCID: PMC5763077.
36. Kuznetsov, V. A.; Makalkin, I. A.; Taylor, M. A.; Perelson, A. S. Nonlinear dynamics of immunogenic tumors: Parameter estimation and global bifurcation analysis. *Bulletin of Mathematical Biology* **1994**, *56(2)*, 295–321. doi: 10.1007/BF02460644. PMID: 8186756.
37. Stein, A.M.; Grupp, S.A.; Levine J.E.; et al. Tisagenlecleucel Model-Based Cellular Kinetic Analysis of Chimeric Antigen Receptor-T Cells. CPT *Pharmacometrics Syst. Pharmacol.* **2019**; *8(5)*, 285-295. doi: 10.1002/psp4.12388. PMID: 30848084.
38. Ghorashian, S.; Kramer, A.M.; Onuoha, S.; Wright, G.; Bartram, J.; Richardson, R.; Albon, S.J.; Casanovas-Company, J.; Castro, F.; Popova, B.; Villanueva, K.; Yeung, J.; Vetharoy, W.; Guvenel, A.; Wawrzyniecka, P.A.; Mekkaoui, L.; Cheung, G.W.; Pinner, D.; Chu, J.; et al. Enhanced CAR T cell expansion and prolonged persistence in pediatric patients with ALL treated with a low-affinity CD19 CAR. *Nature Medicine* **2019**, *25(9)*, 1408–1414. doi: 10.1038/s41591-019-0549-5. PMID: 31477906.
39. Carter, L. L; Fouser, L. A.; Jussif, J.; Fitz, L.; Deng, B.; Wood, C. R.; Collins, M.; Honjo, T.; Freeman, G. J.; Carreno, B. M. PD-1:PD-L inhibitory pathway affects both CD4+ and CD8+ T cells and is overcome by IL-2. *Eur. J. Immunol.* **2002**, *32*, 634–643. doi: 10.4049/jimmunol.1401572. PMID: 25281753
40. Radunskaya, A.; Kim, R.; Woods, T. Mathematical Modeling of Tumor Immune Interactions: A Closer Look at the Role of a PD-L1 Inhibitor in Cancer Immunotherapy *Spora: a Journal of Biomathematics* **2018** *4(1)*, 25–41. doi:10.30707/SPORA4.1Radunskaya.
41. Halkola, A.S.; Parvinen, K.; Kasanen, H.; Mustjoki, S.; Aittokallio, T. Modelling of killer T-cell and cancer cell subpopulation dynamics under immuno- and chemotherapies, *Journal of Theoretical Biology* **2020** *488*, 110136. doi:10.1016/j.jtbi.2019.110136. PMID: 31887273.
42. Benchaib, M.A.; Bouchnita, A.; Volpert, V.; Makhoute, A. Mathematical Modeling Reveals That the Administration of EGF Can Promote the Elimination of Lymph Node Metastases by PD-1/PD-L1 Blockade. *Front Bioeng Biotechnol.* **2019**, *7*:104. doi: 10.3389/fbioe.2019.00104. PMID: 31157216.
43. Khasraw, M.; Reardon ,D.A.; Weller, M.; Sampson, J. H. PD-1 Inhibitors: Do they have a Future in the Treatment of Glioblastoma? *Clin Cancer Res* **2020** *26 (20)*, 5287-5296. doi:10.1158/1078-0432.CCR-20-1135.

44. Stensjøen, A. L.; Solheim, O.; Kvistad, K. A.; Haberg, A. K.; Salvesen, O.; Berntsen, E. M. Growth dynamics of untreated glioblastomas in vivo. *Neuro-Oncology* **2015**, *17(10)*, 1402–1411. doi: 10.1093/neuonc/nov029. PMID: 25758748; PMCID: PMC4578579.
45. Lee, D.W.; Kochenderfer, J.N.; Stetler-Stevenson, M.; et al. T cells expressing CD19 chimeric antigen receptors for acute lymphoblastic leukaemia in children and young adults: a phase 1 dose-escalation trial. *Lancet* **2015**, *385(9967)*, 517-528. doi: 10.1016/S0140-6736(14)61403-3. PMID: 25319501; PMCID: PMC7065359.
46. Fulcher, D.A.; Basten, A. B cell life span: a review. *Immunol. Cell. Biol.* **1997**, *75(5)*, 446-555. doi: 10.1038/icb.1997.69. PMID: 9429891.
47. McGowan, E.; Lin, Q.; Ma, G.; Yin, H.; Chen, S.; Lin, Y. PD-1 disrupted CAR-T cells in the treatment of solid tumors: Promises and challenges. *Biomed Pharmacother.* **2020** *121*,109625. doi: 10.1016/j.biopha.2019.109625. PMID: 31733578.
48. Chen, X.; Jensen, P. E. The role of B lymphocytes as antigen-presenting cells. *Arch. Immunol. Ther. Exp.* **2008**, *56(2)*, 77–83. doi: 10.1007/s00005-008-0014-5. PMID: 18373241.
49. Hirayama, A. V.; Turtle, C. J. Toxicities of CD19 CAR-T cell immunotherapy. *Am. J. Hematol.* **2019**, *94(S1)*, S42–S49. doi: 10.1002/ajh.25445. PMID: 30784102.
50. Siegler, E. L.; Kenderian, S. S. Neurotoxicity and Cytokine Release Syndrome After Chimeric Antigen Receptor T Cell Therapy: Insights Into Mechanisms and Novel Therapies. *Front. Immunol.* **2020** *11*, 1973. https://doi.org/10.3389/fimmu.2020.01973